

Electronic Supplementary Information

Neutral, heteroleptic copper(I)-4*H*-imidazolate complexes: synthesis and characterization of their structural, spectral and redox properties

M. Schulz,* F. Dröge, F. Herrmann-Westendorf, J. Schindler, H. Görls, M. Presselt

martin.schulz.1@uni-jena.de

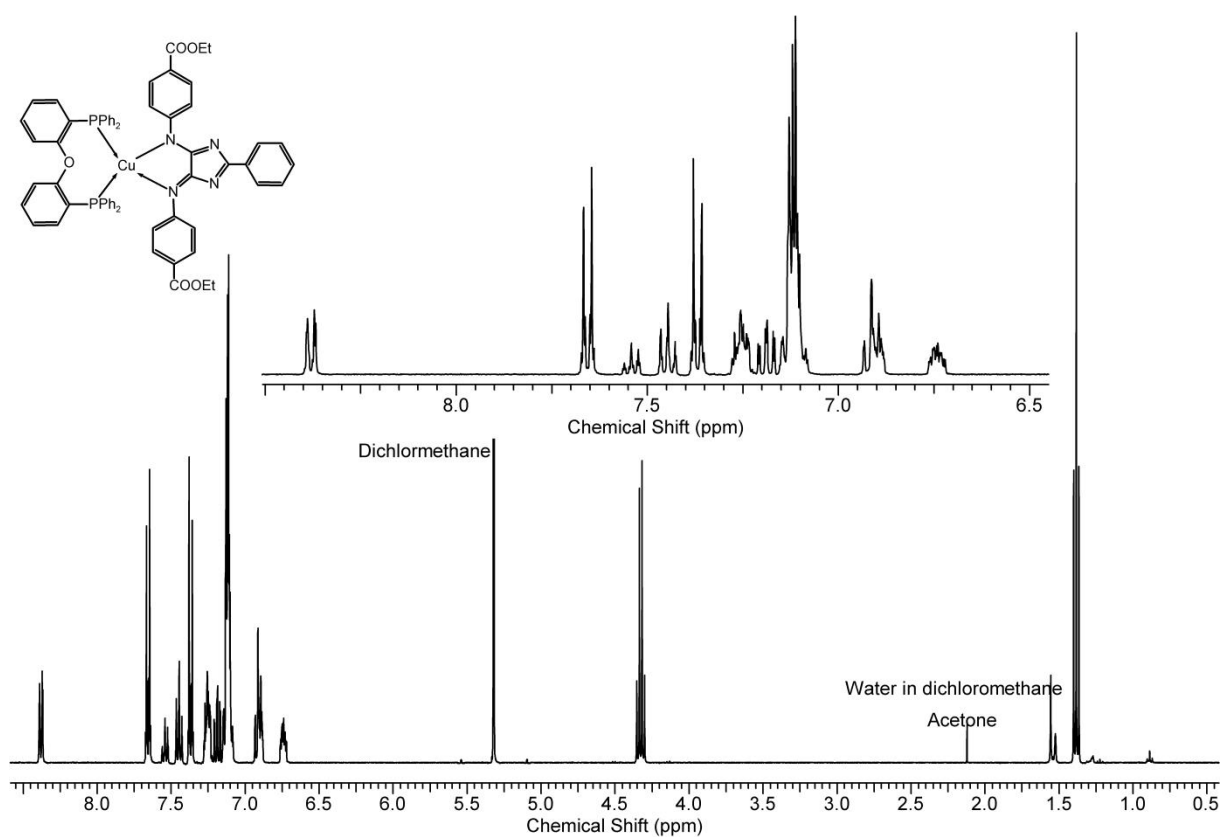


Figure S1 presents the ¹H-NMR spectrum of **CuN1P1** in dichloromethane-D₂ at room temperature. The inset depicts the aromatic region.

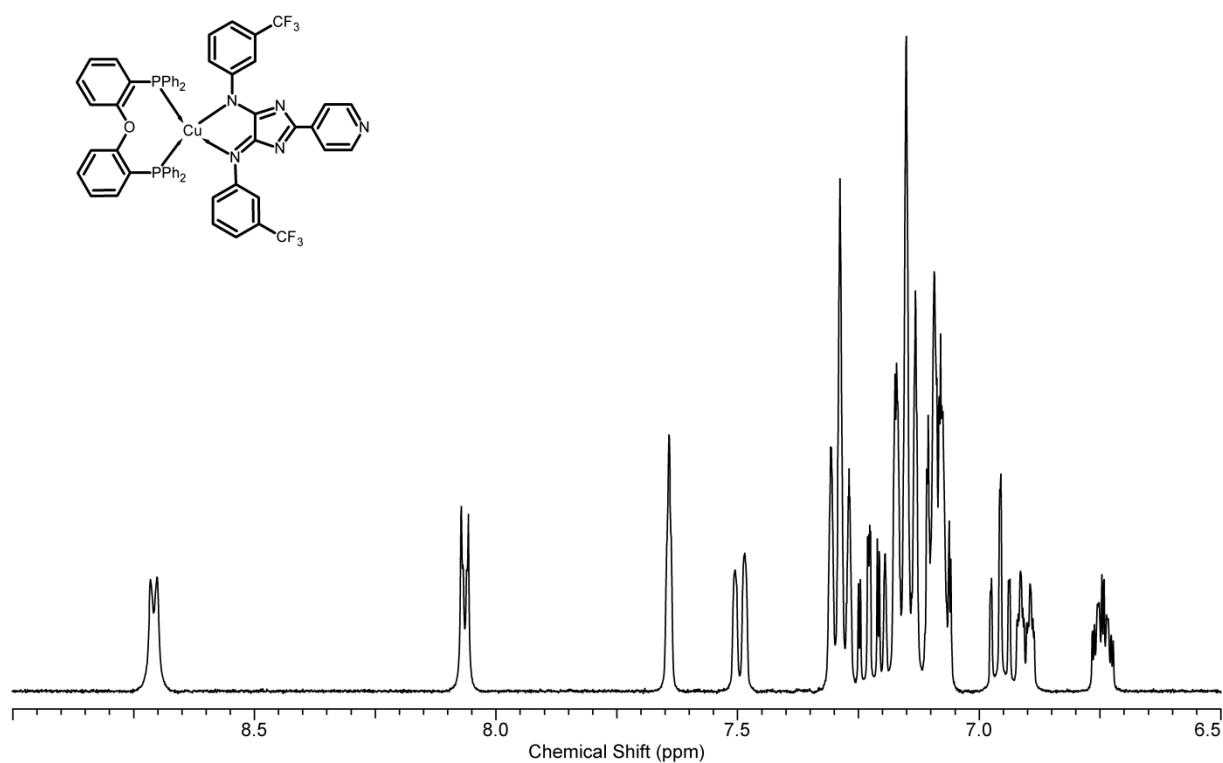


Figure S2 presents the ^1H -NMR spectrum of CuN2P1 in acetonitrile-D3 at room temperature.

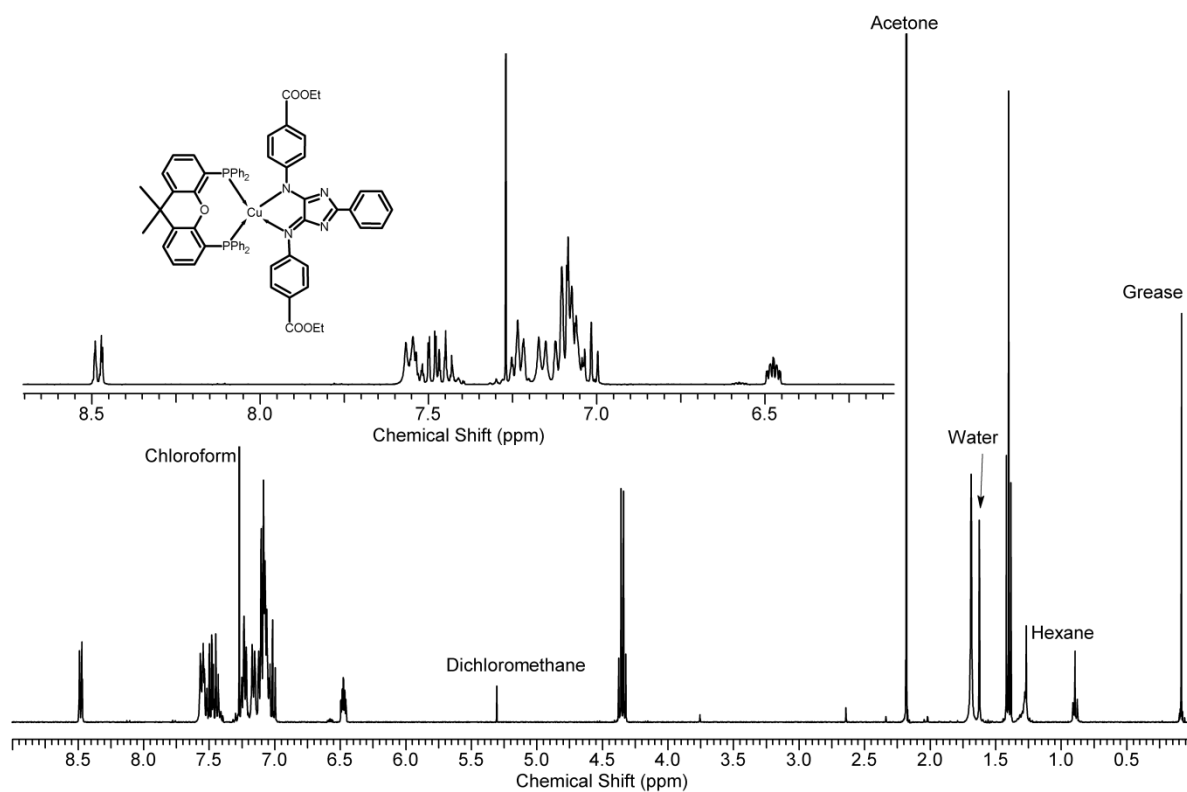


Figure S3 presents the ^1H -NMR spectrum of CuN1P2 in chloroform-D at room temperature. The inset depicts the aromatic region.

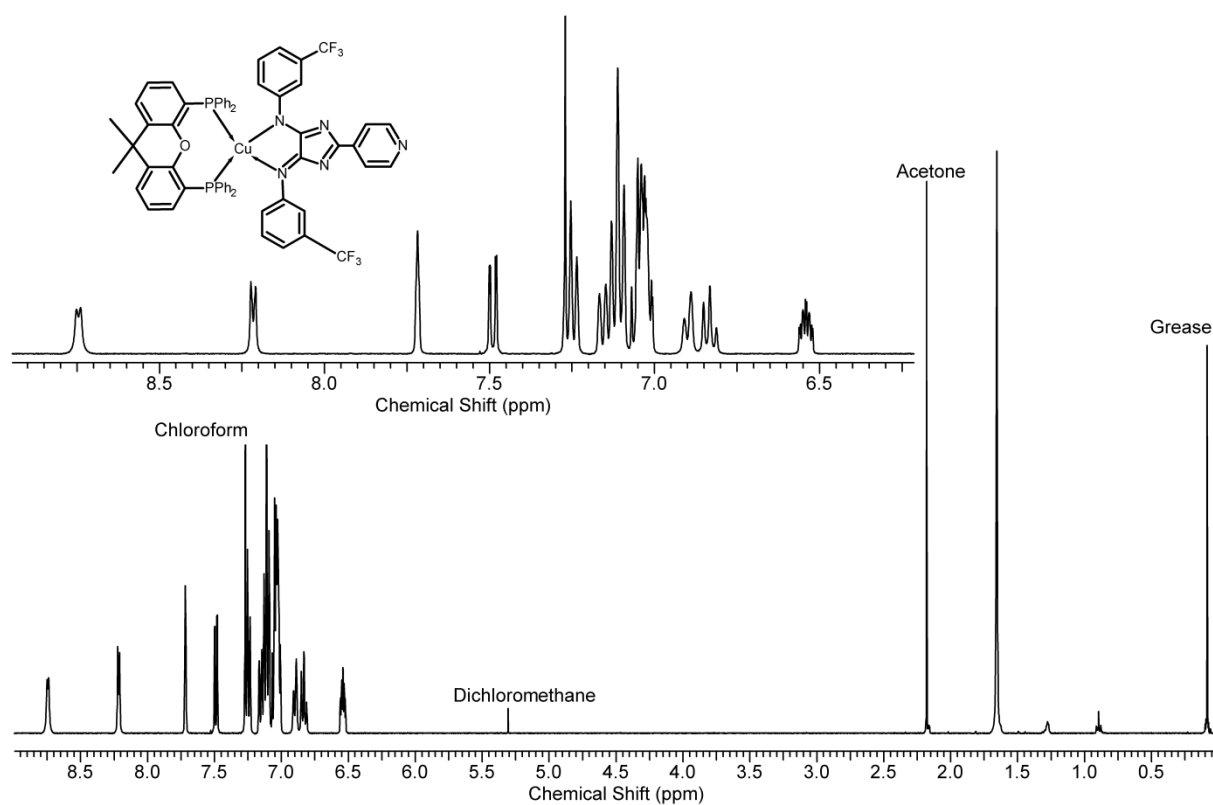


Figure S4 presents the $^1\text{H-NMR}$ spectrum of **CuN2P2** in chloroform-D at room temperature. The inset depicts the aromatic region.

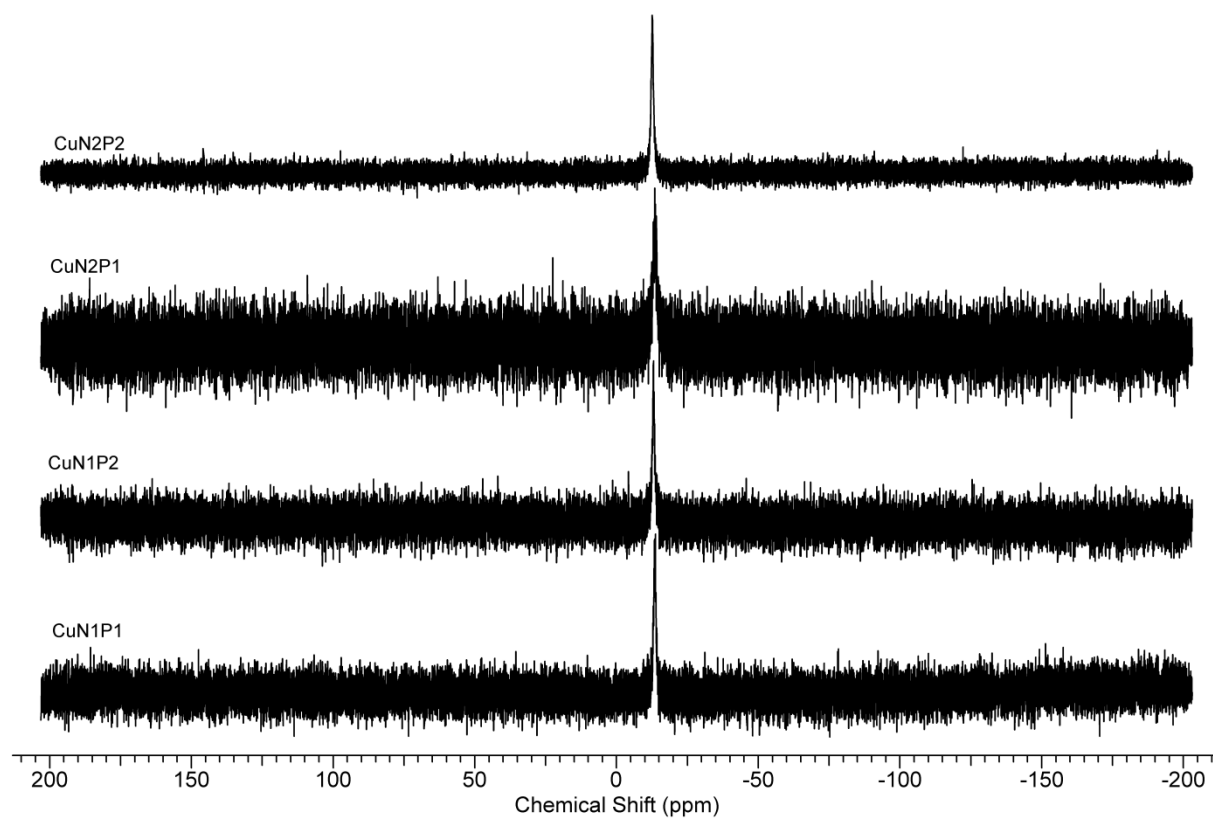


Figure S5 presents the $^{31}\text{P-NMR}$ spectra of the complexes at room temperature.

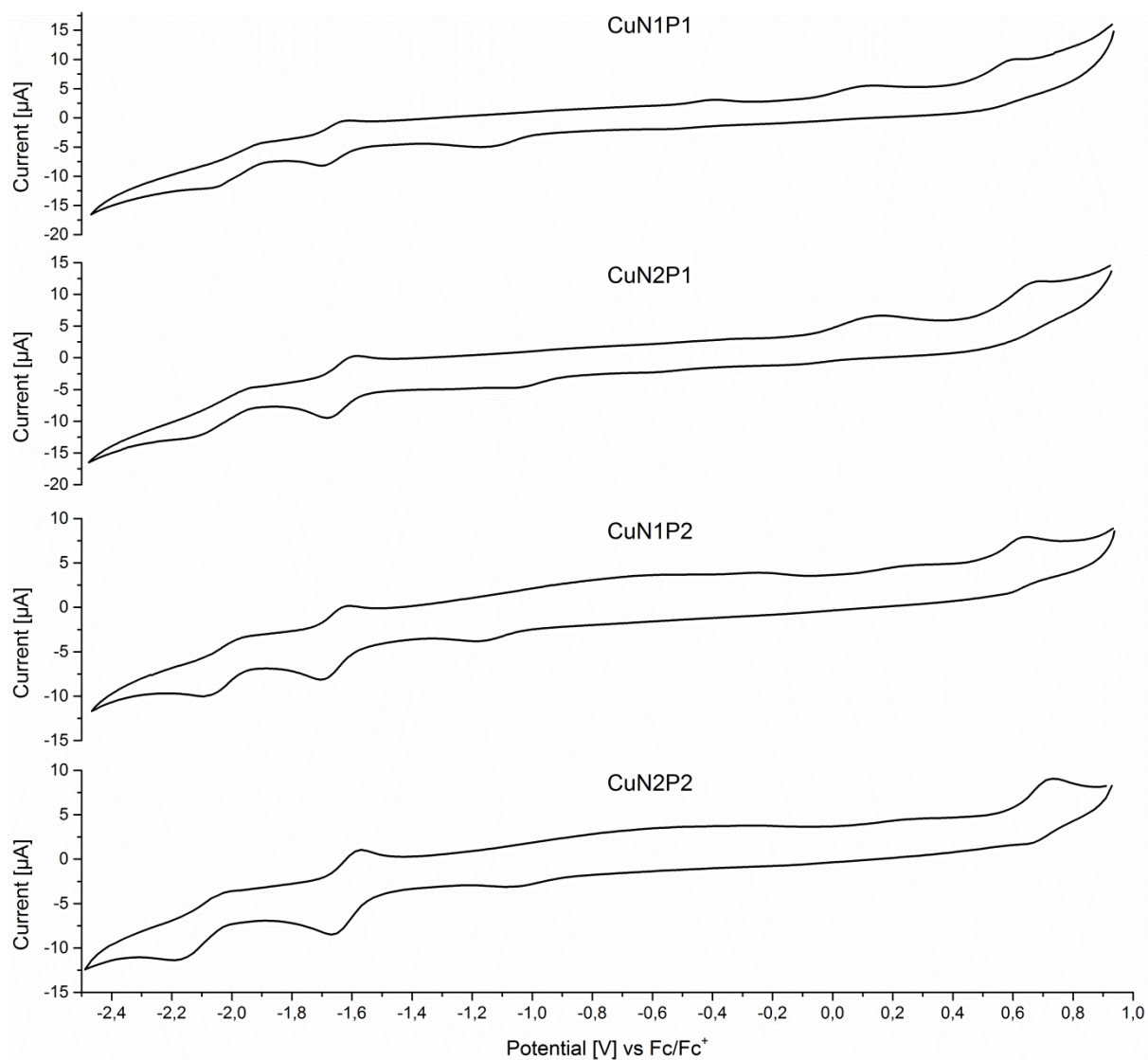


Figure S6 gives the CV curves of the complexes in dichloromethane with 0.1 M tetra-butylammonium BF₄⁻ vs. Fc/Fc⁺ with a scan rate of 0.05 V/s.

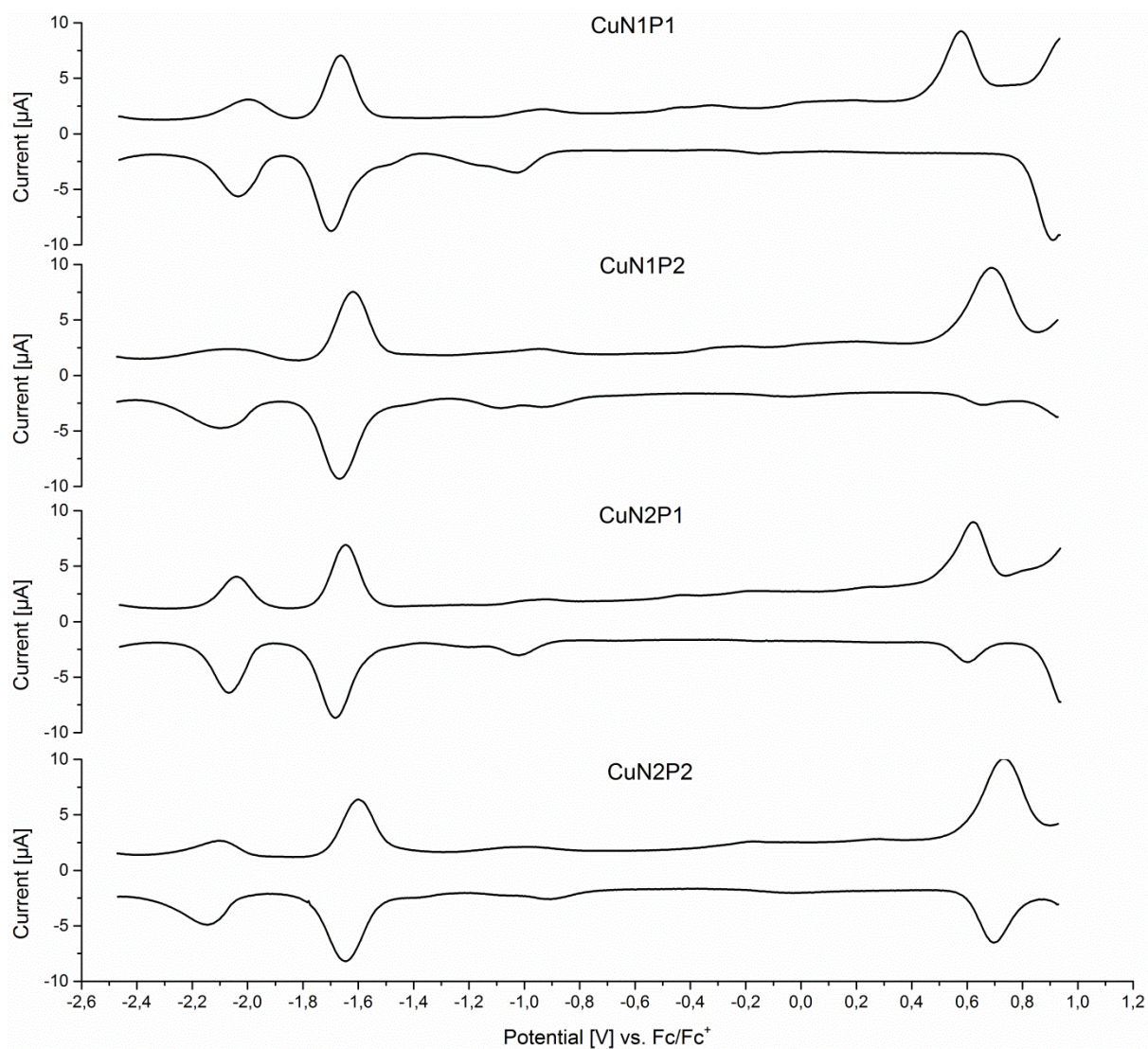


Figure S7 gives the square wave voltammetry curves in dichloromethane with 0.1 M tetra-butylammonium BF_4^- vs. Fc/Fc^+ taken at 64 Hz with a step potential of 5 mV.

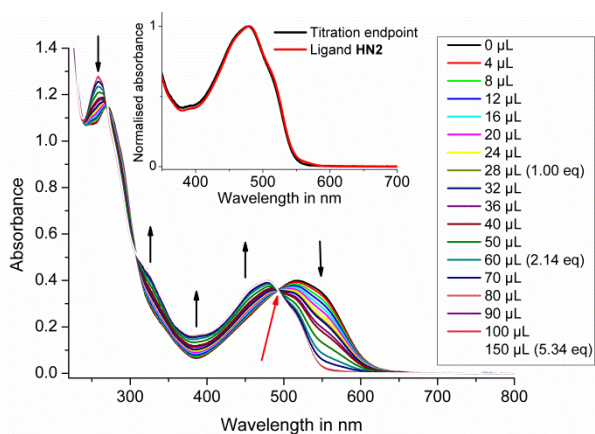
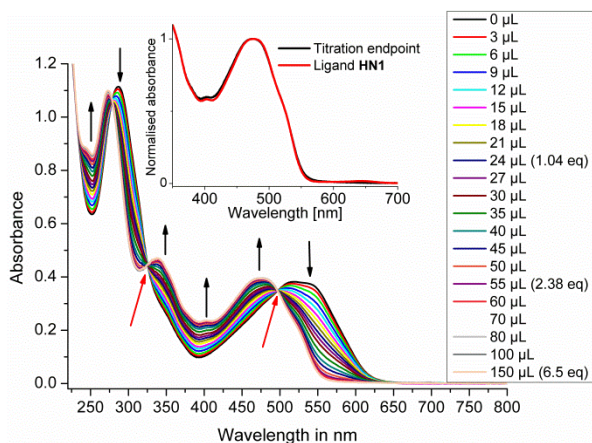
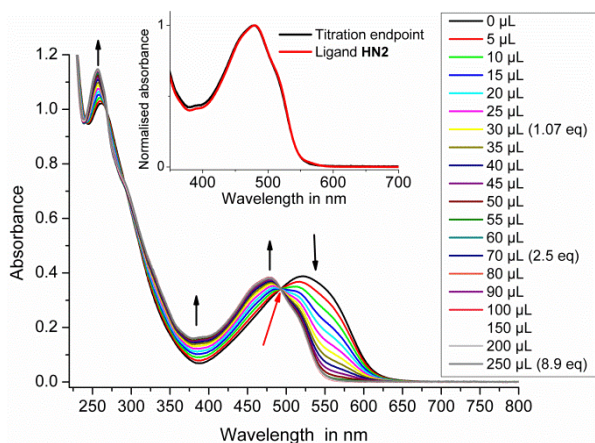


Figure S8 presents the spectral change of solution over the course of titration with trifluoroacetic acid in acetonitrile of: **CuN2P1** (upper left), **CuN1P2** (upper right) and **CuN2P2** (left). The total volumina of TFA in the solution are given together with the molar equivalents, with respect to the complex, in parentheses. Isosbestic points are marked with red arrows. The inset compares the UV-Vis spectrum of the titration endpoint (black) with the UV-Vis spectrum of the neutral *4H*-imidazole ligand in acetonitrile (red), normalised to the absorption maximum.

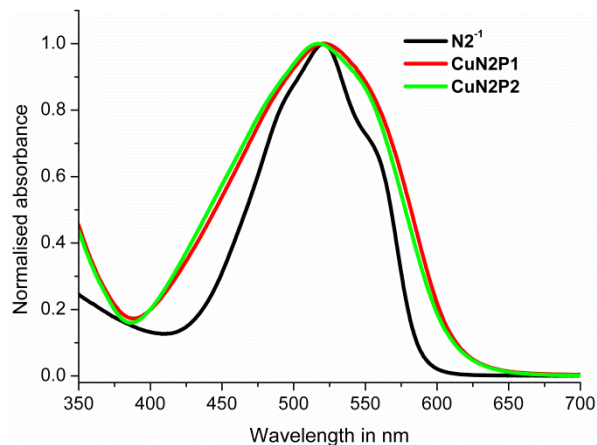
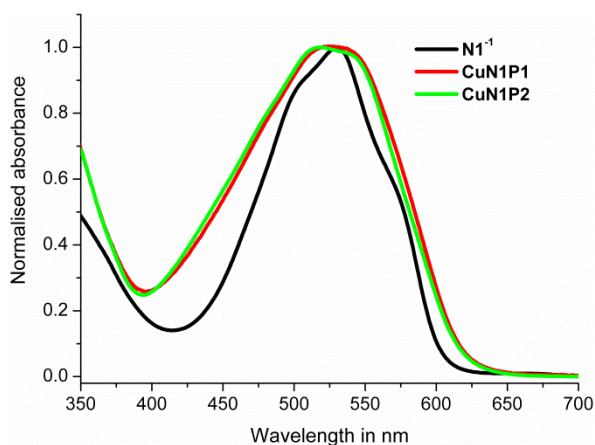


Figure S9 gives a comparison of the UV-Vis absorption spectra between 350-700 nm of the deprotonated *4H*-imidazole ligands (left: **N1⁻**, right **N2⁻**) with the respective complexes.

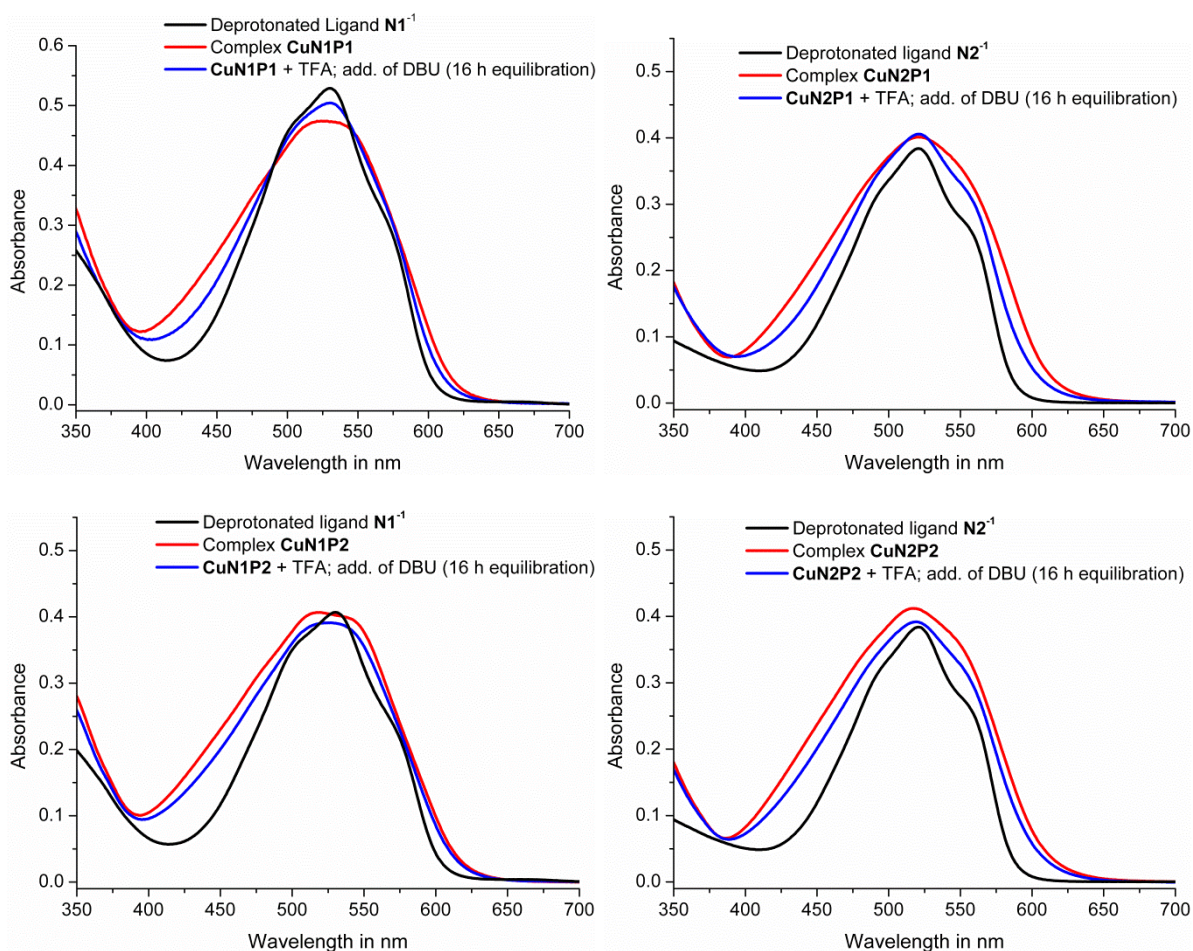


Figure S10 gives a comparison of the UV-Vis absorption between 350-700 nm of the deprotonated 4*H*-imidazole ligands (black), the respective complexes (red) and the spectrum after protonation and decomposition of the complex by addition of excess trifluoroacetic acid (TFA) and subsequent addition of 1,7-diazabicyclo-undec-7-ene (DBU) and 16 h of equilibration in order to recover the complex (blue). The blue spectrum indicates that the complex is not fully recovered after addition of DBU. The extent of recovery reflects the synthetic yields of the complex formation.

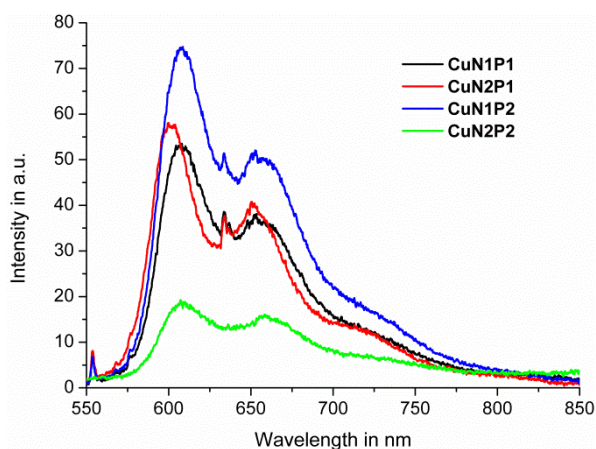


Figure S11 presents the emission spectra of **Cu1P1 – CuN2P2** in dichloromethane solution (not deaerated) upon excitation at 532 nm with a frequency-doubled Nd:YAG laser (5 mW). The weak peaks between 550 and 580nm are Raman bands of the solvent. The small peak at 640 nm is an artefact.

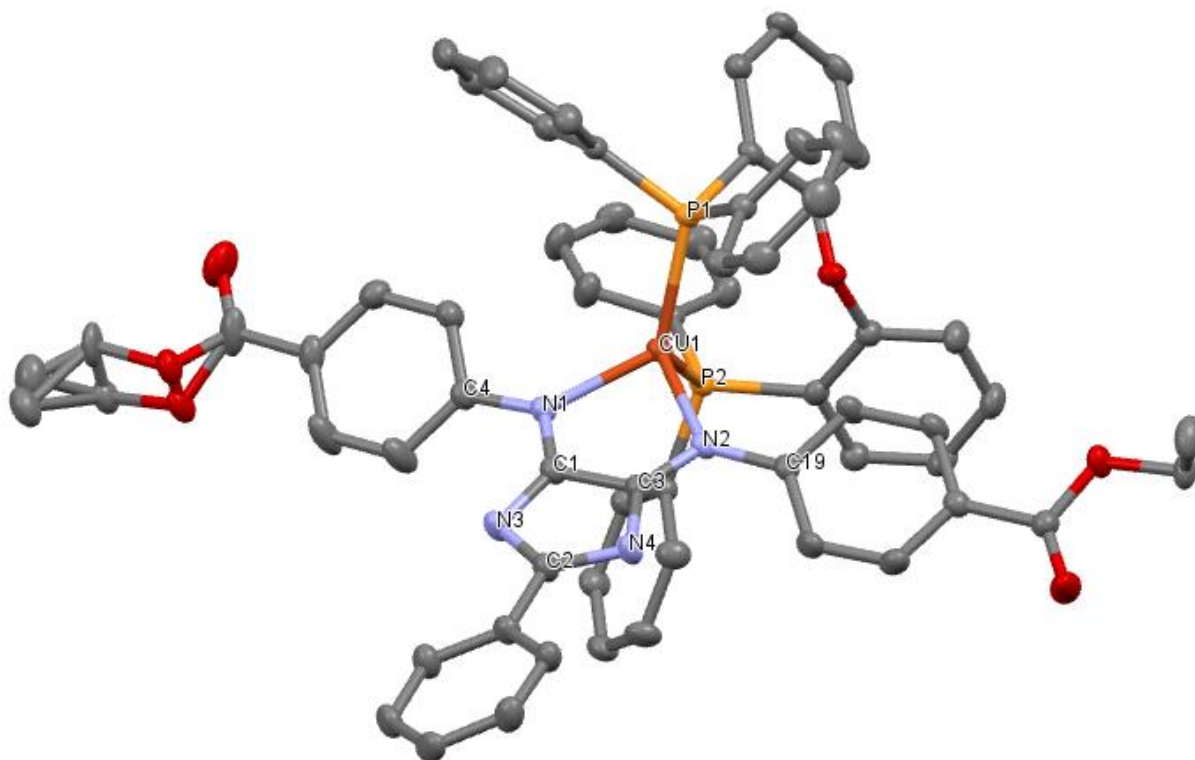


Figure S12 gives the molecular structure of **CuN1P1** with ellipsoids drawn at the 50% probability level. Hydrogen atoms are omitted for clarity. One COOCH₂CH₃ group is disordered.

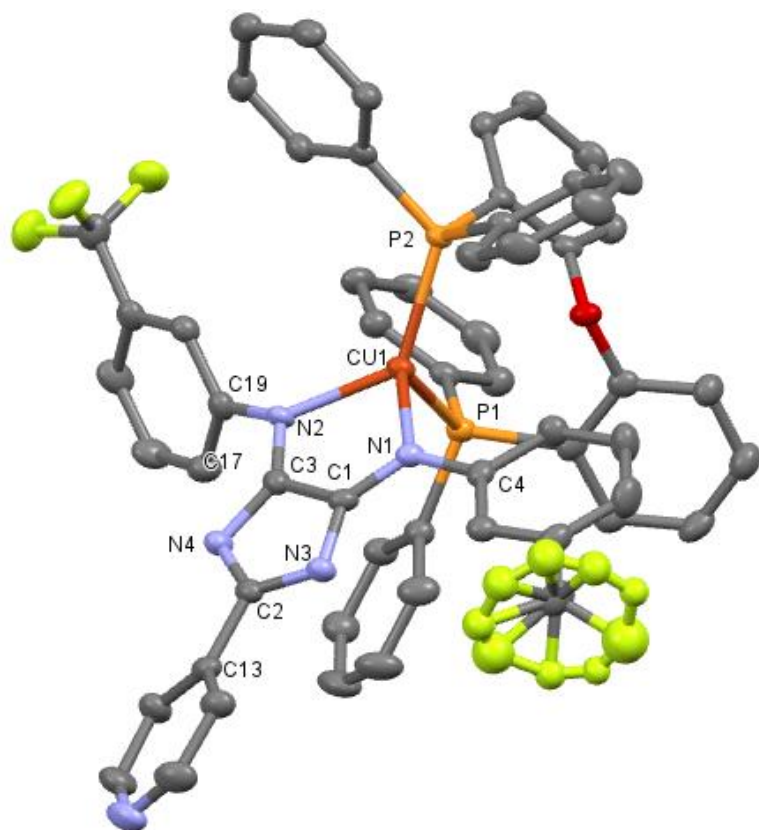


Figure S13 gives the molecular structure of **CuN2P1** with ellipsoids drawn at the 50% probability level. Hydrogen atoms and solvent molecules are omitted for clarity. One CF₃ group is disordered.

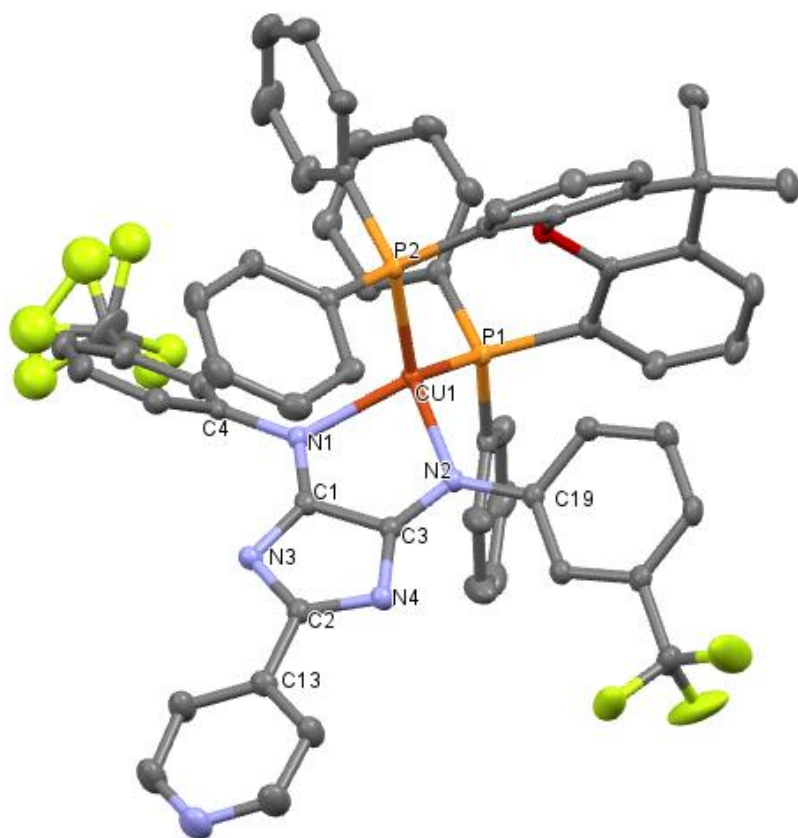


Figure S14 gives the molecular structure of **CuN₂P₂** with ellipsoids drawn at the 50% probability level. Hydrogen atoms are omitted for clarity. One CF₃ group is disordered.

Table S1 Crystal data and refinement details for the X-ray structure determinations of the compounds CuN1P1 - CuN2P2.

Compound	CuN1P1	CuN2P1	CuN1P2	CuN2P2
formula	C ₆₃ H ₅₁ CuN ₄ O ₅ P ₂	C ₅₈ H ₄₀ CuF ₆ N ₅ OP ₂ , C ₃ H ₆ O[*]	C ₆₆ H ₅₅ CuN ₄ O ₅ P ₂ , CH ₂ Cl ₂	C ₆₁ H ₄₄ CuF ₆ N ₅ OP ₂
fw (g·mol ⁻¹)	1069.56	1120.51[*]	1194.55	1102.49
°C	-140(2)	-140(2)	-140(2)	-140(2)
crystal system	triclinic	triclinic	triclinic	monoclinic
space group	P $\bar{1}$	P $\bar{1}$	P $\bar{1}$	P 2 ₁ /c
a/ Å	14.1809(3)	12.8088(4)	12.2239(2)	11.7550(1)
b/ Å	14.5825(3)	13.5384(5)	16.2189(3)	19.8468(3)
c/ Å	15.1972(3)	19.2330(7)	16.5242(3)	22.9847(4)
α /°	70.329(1)	88.555(2)	63.069(1)	90
β /°	63.513(1)	71.411(2)	85.486(1)	100.928(1)
γ /°	77.344(1)	69.456(2)	85.350(1)	90
V/Å ³	2639.77(9)	2946.03(18)	2907.91(9)	5265.07(13)
Z	2	2	2	4
ρ (g·cm ⁻³)	1.346	1.263[*]	1.364	1.391
μ (cm ⁻¹)	5.3	4.89[*]	5.78	5.45
measured data	20136	11717	22742	35568
data with I > 2 σ (I)	10120	9397	10487	10217
unique data (R _{int})	11670/0.0257	11717/0.0413	12546/0.0362	11970/0.0389
wR ₂ (all data, on F ²) ^{a)}	0.0883	0.1176	0.1430	0.1113
R ₁ (I > 2 σ (I)) ^{a)}	0.0419	0.0597	0.0552	0.0491
S ^{b)}	1.097	1.075	1.058	1.048
Res. dens./e·Å ⁻³	0.388/-0.416	0.723/-0.615	0.879/-1.100	1.439/-1.120
absorpt method	multi-scan	multi-scan	multi-scan	multi-scan
absorpt corr T _{min} /max	0.7069/0.7456	0.6909/0.7456	0.6991/0.7456	0.7203/0.7456
CCDC No.	1432665	1432667	1432666	1432668

[*] derived parameters do not contain the contribution of the disordered solvent.

^{a)} Definition of the R indices: $R_1 = (\sum ||F_o| - |F_c||) / \sum |F_o|$;

$wR_2 = \{\sum [w(F_o^2 - F_c^2)^2] / \sum [w(F_o^2)^2]\}^{1/2}$ with $w^{-1} = \sigma^2(F_o^2) + (aP)^2 + bP$; $P = [2F_c^2 + \text{Max}(F_o^2)]/3$;

^{b)} $S = \{\sum [w(F_o^2 - F_c^2)^2] / (N_o - N_p)\}^{1/2}$.

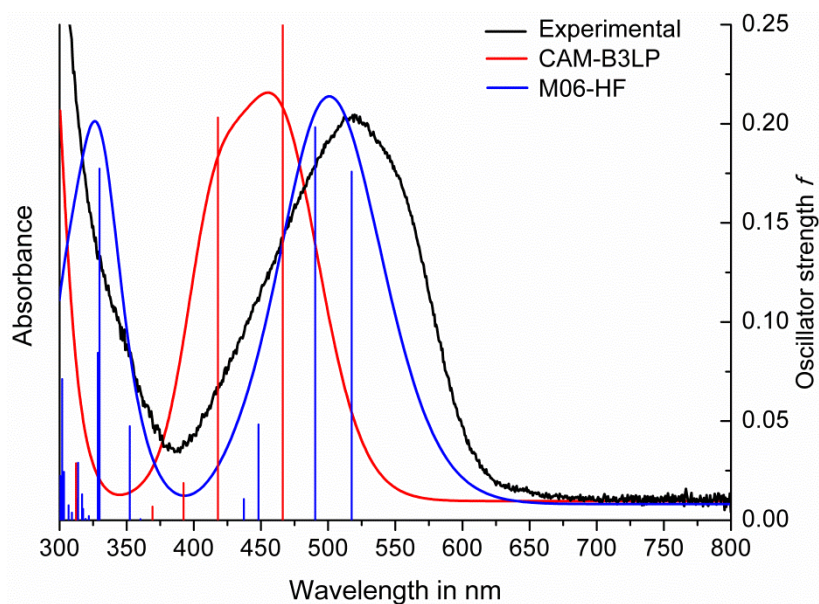


Figure S15 gives a comparison between the experimental UV-Vis absorption band of **CuN2P2** and the calculated spectra (CAM-B3LYP vs. M06-HF). The vertical bars indicate the calculated transitions. Calculations of the first 20 singlet transitions were made on the TD-DFT level of theory using either the CAM-B3LYP¹ functional or M06-HF² with the MDF10 basis set for copper and 6-31G(d) for the remainder. Convolution of the simulated spectra was accomplished with the GaussSum³ program using Gauss functions for each transition with FWHM = 3000 cm⁻¹.

Table S2 presents the percent contributions to selected frontier orbitals of **CuN2P2** in the singlet ground state (M06)

No.	MO	eV	Sym.	Cu	N-Aryl	Imidazole	2-Aryl	Phosphane
282	L+3	-0.75	A	43	5	4	12	36
281	L+2	-0.83	A	3	6	2	4	85
280	L+1	-1.0	A	3	3	1	0	93
279	LUMO	-2.57	A	2	17	60	20	2
278	HOMO	-5.83	A	31	5	12	1	51
277	H-1	-5.95	A	9	31	51	0	9
276	H-2	-6.45	A	35	3	15	0	47
275	H-3	-6.49	A	43	23	26	1	7

Table S3 presents the percent contributions to selected frontier orbitals of **CuN2P2** in the singlet ground state (CAM-B3LYP)

No.	MO	eV	Sym.	Cu	N-Aryl	Imidazole	2-Aryl	Phosphane
282	L+3	0.45	A	2	18	12	32	36
281	L+2	0.36	A	1	5	1	3	89
280	L+1	0.17	A	2	3	0	0	94
279	LUMO	-1.59	A	1	17	61	19	2
278	HOMO	-6.81	A	18	21	38	1	23
277	H-1	-6.88	A	22	14	29	1	33
276	H-2	-7.52	A	35	4	13	0	46
275	H-3	-7.56	A	44	22	23	1	11

References

1. T. Yanai, D. P. Tew, and N. C. Handy, *Chem. Phys. Lett.*, 2004, **393**, 51–57.
2. Y. Zhao and D. G. Truhlar, *Theor. Chem. Acc.*, 2008, **120**, 215–241.
3. N. M. O’Boyle, A. L. Tenderholt, and K. M. Langner, *J. Comput. Chem.*, 2008, **29**, 839–845.